

## Dear Author

Here are the proofs of your article.

- You can submit your corrections **online**, via **e-mail** or by **fax**.
- For **online** submission please insert your corrections in the online correction form. Always indicate the line number to which the correction refers.
- You can also insert your corrections in the proof PDF and **email** the annotated PDF.
- For **fax** submission, please ensure that your corrections are clearly legible. Use a fine black pen and write the correction in the margin, not too close to the edge of the page.
- Remember to note the **journal title**, **article number**, and **your name** when sending your response via e-mail or fax.
- **Check** the metadata sheet to make sure that the header information, especially author names and the corresponding affiliations are correctly shown.
- **Check** the questions that may have arisen during copy editing and insert your answers/corrections.
- **Check** that the text is complete and that all figures, tables and their legends are included. Also check the accuracy of special characters, equations, and electronic supplementary material if applicable. If necessary refer to the *Edited manuscript*.
- The publication of inaccurate data such as dosages and units can have serious consequences. Please take particular care that all such details are correct.
- Please **do not** make changes that involve only matters of style. We have generally introduced forms that follow the journal's style.
- Substantial changes in content, e.g., new results, corrected values, title and authorship are not allowed without the approval of the responsible editor. In such a case, please contact the Editorial Office and return his/her consent together with the proof.
- If we do not receive your corrections **within 48 hours**, we will send you a reminder.
- Your article will be published **Online First** approximately one week after receipt of your corrected proofs. This is the **official first publication** citable with the DOI. **Further changes are, therefore, not possible.**
- The **printed version** will follow in a forthcoming issue.

### Please note

After online publication, subscribers (personal/institutional) to this journal will have access to the complete article via the DOI using the URL:

<http://dx.doi.org/10.1007/s00367-016-0481-3>

If you would like to know when your article has been published online, take advantage of our free alert service. For registration and further information, go to:

<http://www.link.springer.com>.

Due to the electronic nature of the procedure, the manuscript and the original figures will only be returned to you on special request. When you return your corrections, please inform us, if you would like to have these documents returned.

**Metadata of the article that will be visualized in OnlineFirst**

1	Article Title	<b>Sequential development of tidal ravinement surfaces in macro- to hypertidal estuaries with high volcaniclastic input: the Miocene Puerto Madryn Formation (Patagonia, Argentina)</b>	
2	Article Sub- Title		
3	Article Copyright - Year	<b>Springer-Verlag Berlin Heidelberg 2016 (This will be the copyright line in the final PDF)</b>	
4	Journal Name	Geo-Marine Letters	
5		Family Name	<b>Scasso</b>
6		Particle	
7		Given Name	<b>Roberto A.</b>
8		Suffix	
9	Corresponding Author	Organization	Universidad de Buenos Aires
10		Division	IGeBA-Departamento de Cs. Geológicas, Facultad de Ciencias Exactas y Naturales
11		Address	Ciudad Universitaria, Pabellón 2, 1° Piso (1428), Ciudad Autónoma de Buenos Aires
12		e-mail	rscasso@gl.fcen.uba.ar
13		Family Name	<b>Cuitiño</b>
14		Particle	
15		Given Name	<b>José I.</b>
16		Suffix	
17	Author	Organization	Instituto Patagónico de Paleontología y Geología (CCT CENPAT-CONICET)
18		Division	
19		Address	Boulevard Brown N° 2915, Puerto Madryn, Chubut
20		e-mail	
21		Received	6 June 2016
22	Schedule	Revised	
23		Accepted	31 October 2016
24	Abstract	The late Miocene beds of the Puerto Madryn Formation (Provincia del Chubut, Argentina) are formed by shallow marine and estuarine sediments. The latter include several tidal-channel infills well exposed on the cliffy coast of the Peninsula Valdés. The Bahía Punta Fósil and Cerro Olazábal paleochannels are end members of	

these tidal channels and show a fining-upward infilling starting with intraformational channel lag conglomerates above deeply erosional surfaces interpreted as fluvial ravinement surfaces (the erosion surface formed in the purely fluvial or the fluvially dominated part of the estuary, where erosion is driven by fluvial processes). These are overlain and eventually truncated (and suppressed) by the tidal ravinement surface (TRS), in turn covered with high-energy, bioclastic conglomerates mostly formed in the “tidally dominated/fluvially influenced” part of an estuary. Above, large straight or arcuate point bars with alternatively sandy/muddy seasonal beds and varying trace and body fossil contents were deposited from the freshwater fluvially dominated to saline-water tidally dominated part of the estuary. The upper channel infill is formed by cross-bedded sands with mud drapes and seaward-directed paleocurrents, together with barren, volcanoclastic sandy to muddy heterolithic seasonal rhythmites, both deposited in the fluvially dominated part of the estuary. Volcanic ash driven by the rivers after large explosive volcanic eruptions on land resulted in sedimentation rates as high as 0.9 m per year, preserving (through burial) the morphology of tidal channels and TRSs. The channel deposits were formed in a tide-dominated, macrotidal to hypertidal open estuary with well-developed TRSs resulting from strong tidal currents deeply scouring into the transgressive filling of the channels and eventually cutting the fluvial ravinement surface. The TRSs extended upstream to the inner part of the estuary during long periods of low sedimentation rates, extended channel migration and sediment bypass, interrupted by transient, high volcanoclastic input. The tidal channels of the Puerto Madryn Formation constitute a unique example of estuary sedimentation with pulsed sediment supply in a macrotidal to hypertidal estuary.

---

25 Keywords  
separated by ' - '

---

26 Foot note information      Responsible editor: B.W. Flemming

4  
5  
6 **Sequential development of tidal ravinement surfaces in macro-  
to hypertidal estuaries with high volcanoclastic input: the Miocene  
Puerto Madryn Formation (Patagonia, Argentina)**7 **Roberto A. Scasso<sup>1</sup> · José I. Cuitiño<sup>2</sup>**  
89 Received: 6 June 2016 / Accepted: 31 October 2016  
10 © Springer-Verlag Berlin Heidelberg 201611 **Abstract** The late Miocene beds of the Puerto Madryn  
12 Formation (Provincia del Chubut, Argentina) are formed  
13 by shallow marine and estuarine sediments. The latter  
14 include several tidal-channel infills well exposed on the  
15 cliffy coast of the Peninsula Valdés. The Bahía Punta  
16 Fósil and Cerro Olazábal paleochannels are end members  
17 of these tidal channels and show a fining-upward infilling  
18 starting with intraformational channel lag conglomerates  
19 above deeply erosional surfaces interpreted as fluvial  
20 ravinement surfaces (the erosion surface formed in the  
21 purely fluvial or the fluvially dominated part of the estu-  
22 ary, where erosion is driven by fluvial processes). These  
23 are overlain and eventually truncated (and suppressed) by  
24 the tidal ravinement surface (TRS), in turn covered with  
25 high-energy, bioclastic conglomerates mostly formed in  
26 the “tidally dominated/fluvially influenced” part of an estu-  
27 ary. Above, large straight or arcuate point bars with  
28 alternatively sandy/muddy seasonal beds and varying  
29 trace and body fossil contents were deposited from the  
30 freshwater fluvially dominated to saline-water tidally  
31 dominated part of the estuary. The upper channel infill  
32 is formed by cross-bedded sands with mud drapes andseaward-directed paleocurrents, together with barren, 33  
volcanoclastic sandy to muddy heterolithic seasonal 34  
rhythmites, both deposited in the fluvially dominated part 35  
of the estuary. Volcanic ash driven by the rivers after large 36  
explosive volcanic eruptions on land resulted in sedimen- 37  
tation rates as high as 0.9 m per year, preserving (through 38  
burial) the morphology of tidal channels and TRSs. The 39  
channel deposits were formed in a tide-dominated, 40  
macrotidal to hypertidal open estuary with well- 41  
developed TRSs resulting from strong tidal currents deep- 42  
ly scouring into the transgressive filling of the channels 43  
and eventually cutting the fluvial ravinement surface. The 44  
TRSs extended upstream to the inner part of the estuary 45  
during long periods of low sedimentation rates, extended 46  
channel migration and sediment bypass, interrupted by 47  
transient, high volcanoclastic input. The tidal channels of 48  
the Puerto Madryn Formation constitute a unique example 49  
of estuary sedimentation with pulsed sediment supply in a 50  
macrotidal to hypertidal estuary. 52**Introduction** 53The nature of discontinuity surfaces in estuaries and their 54  
relationships to sea-level changes have been studied since 55  
the advent of sequence stratigraphy, but their unambigu- 56  
ous identification in ancient deposits is still difficult. The 57  
study of Recent and Holocene infillings in tide-dominated 58  
estuaries (e.g., Tessier et al. 2012) is helpful because it 59  
involves short and well-constrained periods of time, and 60  
sea-level change is limited and well known. Identification 61  
of the tidal ravinement surface (TRS) is crucial to under- 62  
stand the evolution of tide-dominated (and some mixed 63  
energy) estuaries (Chaumillon et al. 2010). TRSs are 64  
formed at the erosional base of tidal channels (Allen and 65

Responsible editor: B.W. Flemming

✉ Roberto A. Scasso  
rscasso@gl.fcen.uba.ar<sup>1</sup> IGeBA-Departamento de Cs. Geológicas, Facultad de Ciencias Exactas y Naturales, Universidad de Buenos Aires, Ciudad Universitaria, Pabellón 2, 1° Piso (1428), Ciudad Autónoma de Buenos Aires, Argentina<sup>2</sup> Instituto Patagónico de Paleontología y Geología (CCT CENPAT-CONICET), Boulevard Brown N° 2915, Puerto Madryn, Chubut, Argentina

66 Posamentier 1993) by upward and backward  
 67 (retrogradational) migration of the estuarine system  
 68 (Boyd et al. 1992; Dalrymple et al. 1992), and may extend  
 69 throughout tide-dominated estuaries (Zaitlin et al. 1994;  
 70 Tessier 2012). The depth of tidal ravinement is related to  
 71 the tidal range and current energy in tidal channels within  
 72 tidally dominated estuaries. The TRS may erode very  
 73 deep in some macrotidal or hypertidal settings, eventually  
 74 cutting the transgressive surface (e.g., Allen and  
 75 Posamentier 1994) and becoming the main discontinuity  
 76 within the infill of incised valleys. Furthermore, they may  
 77 cut the subaerial incision surface in starved estuaries  
 78 (Chaumillon et al. 2010; Tessier 2012). In these tracts,  
 79 the TRS becomes itself (and is coplanar to) the sequence  
 80 boundary.

81 In tide-dominated estuaries, autocyclic processes (e.g., chan-  
 82 nel migration) interact and overlap with allocyclic processes  
 83 (e.g., sea-level changes) to produce complex sediment bodies  
 84 bounded by erosion surfaces. Most of these sediment bodies  
 85 are lensoidal and result from sedimentation in channels with  
 86 extended or limited lateral migration. They typically range  
 87 from hundreds of meters to a few kilometers wide and a few  
 88 meters to several tens of meters thick. These laterally discon-  
 89 tinuous sediment bodies are difficult to trace and correlate in  
 90 outcrops. Conversely, they can be traced and correlated to dis-  
 91 continuities with high-resolution seismic techniques in the sub-  
 92 surface (e.g., Ashley and Sheridan 1994; Maynard et al. 2010)  
 93 where direct observation of the sedimentary rocks is limited.  
 94 The potential for preservation of estuarine sedimentary bodies  
 95 is primarily controlled by tidal accommodation, defined by the  
 96 depth of the main tidal channel belt (Tessier 2012).

97 On the other hand, high sedimentation rates and rapid ag-  
 98 gradation in tidal channels within macro- to hypertidal areas  
 99 promote the abundance of tidal rhythmites under transgressive  
 100 conditions (Archer and Greb 2012; Archer 2013). Aggradational  
 101 conditions are dominant during volcanic erup-  
 102 tive periods (Smith 1991), and may lead to the instantaneous  
 103 preservation of channel geometry in transitional settings  
 104 (Cuitiño and Scasso 2013).

105 Superb exposures of the tide-dominated estuarine deposits  
 106 of the late Miocene Puerto Madryn Formation (Haller 1979;  
 107 Scasso and del Río 1987) on coastal cliffs and gullies along  
 108 the coasts of Golfo Nuevo and Golfo San José in the Peninsula  
 109 Valdés (Provincia del Chubut, Argentina; see Fig. 1) have  
 110 allowed detailed paleoenvironmental analyses and the recon-  
 111 struction of the 3-D geometry of channel fills as well as tracing  
 112 erosion surfaces along tens of kilometers (Scasso et al. 2012,  
 113 2014, 2015a, 2015b), but an integrated sedimentological,  
 114 paleoenvironmental and sequence-stratigraphical analysis  
 115 was still missing. In order to achieve this, two stratigraphic  
 116 intervals, representative of different parts of ancient estuarine  
 117 systems with channel deposits and prominent erosion sur-  
 118 faces, were selected. This allowed reconstruction of the

geometric and temporal relations of the subaerial (fluvial  
 ravinement) and TRS surfaces in incised valleys with high-  
 energy tidal channels within macro- to hypertidal systems  
 during times of sea-level rising. Neither the stratigraphic rela-  
 tion of both surfaces nor the aggradational volcanoclastic  
 infilling has been documented in estuarine ancient deposits  
 such as those of the Puerto Madryn Formation. Moreover,  
 the influence of volcanoclastic input in the preservation of  
 the irregular discontinuity surfaces is analyzed.

**Geological setting**

The Cenozoic succession of the Puerto Madryn–Península  
 Valdés region comprises flat-lying strata on top of a  
 Jurassic volcanic basement (Scasso et al. 2010). The  
 Cenozoic succession wedges out to the west but its thick-  
 ness greatly increases on the Atlantic shelf (Marinelli and  
 Franzín 1996; Caramés et al. 2004). The integrated strat-  
 igraphic column derived from surface studies (Fig. 2)  
 starts with the early Miocene Gaiman Formation, which  
 is covered by yellowish-rusty brown late Miocene beds of  
 the Puerto Madryn Formation (Haller 1979). The Puerto  
 Madryn Formation is assigned to the late Miocene (10  
 ±0.3 Ma, Tortonian; Zinsmeister et al. 1981; Scasso  
 et al. 2001). This age assignment is supported by infor-  
 mation on malacofauna (Martínez and del Río 2002; del  
 Río 2004), palynology (Palazzesi and Barreda 2004), for-  
 aminifers (Marengo 2015) and mammals (Dozo et al.  
 2010).

The Puerto Madryn Formation crops out extensively in the  
 Península Valdés (Fig. 1), and it is nicely exposed at the coast-  
 al cliffs as well as inland in some gullies. It is formed by more  
 than 150 m of shallow-marine heterolithic and cross-bedded  
 volcanoclastic sandstones, muddy sandstones, and sandy  
 shales interbedded with whitish tuffs and distinctive shell beds  
 (coquinas). The Puerto Madryn Formation locally represents  
 the late Miocene marine transgression that covered a large part  
 of Argentina (and South America), forming a shallow sea  
 connected to the Atlantic Ocean known in the literature as  
 the “Enterriense” sea (e.g., Scasso and del Río 1987). A  
 southern branch of the “Enterriense” sea formed a wide bay  
 that penetrated westward in the Península Valdés region and  
 was subjected to strong tidal currents. Facies distributions and  
 paleocurrent patterns point to a provenance and sediment dis-  
 persion from the south and southwest to north and northeast  
 (Scasso and del Río 1987).

**Sequence stratigraphy and paleoenvironments: synthesis from previous work**

The Puerto Madryn Formation lies on a regionally exten-  
 sive ravinement surface cut on older marine strata of the

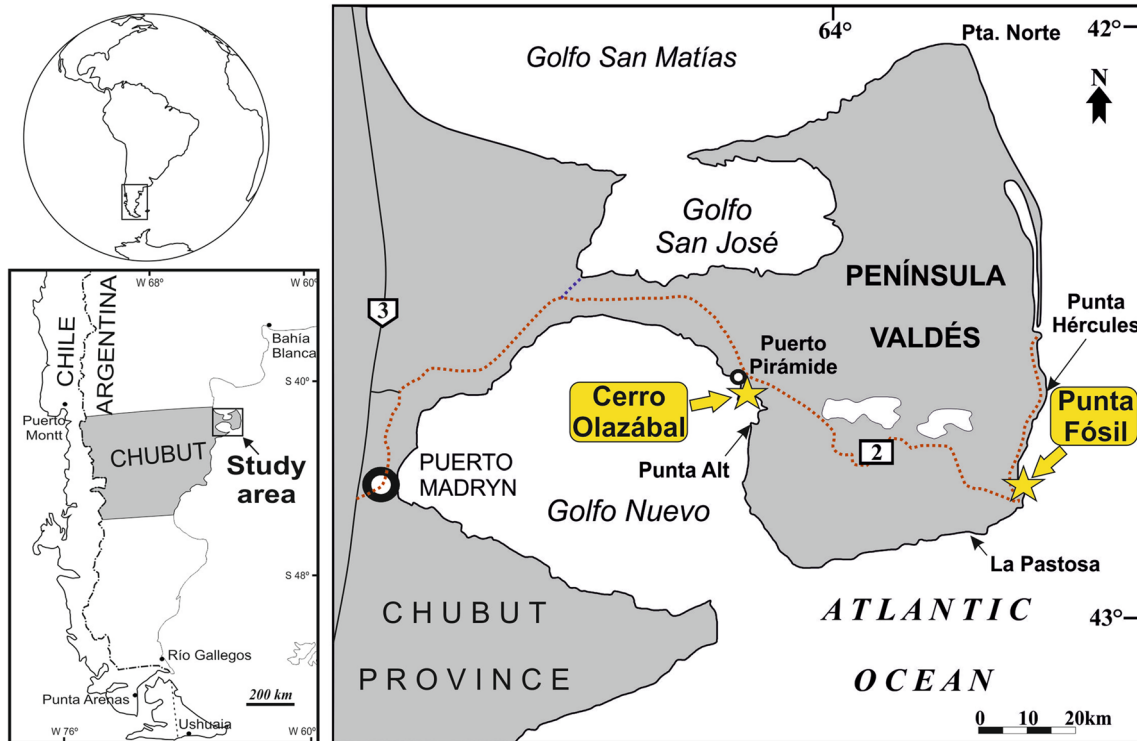


**Fig. 1** Location sketch map of the Península Valdés in Patagonia, with location of the study sites and other nearby sites referred to in the text. National road 3 and provincial road 2 are also indicated

167 early Miocene Gaiman Formation (Scasso and del Río  
 168 1987). Previous work subdivided the Puerto Madryn  
 169 Formation into three vertically stacked units called (from  
 170 base to top) the transgressive phase, the maximum  
 171 highstand phase, and the regressive phase (del Río et al.  
 172 2001). The maximum highstand phase refers to deposits  
 173 that accumulated when the sea level was at its maximum,  
 174 and is separated from the underlying transgressive phase  
 175 by the maximum flooding surface (del Río et al. 2001).  
 176 From a standard sequence stratigraphic point of view, the  
 177 strata forming the unit can be organized as a third-order  
 178 transgressive-regressive (T-R) sequence, in which the  
 179 transgressive phase of del Río et al. (2001) corresponds  
 180 to the transgressive systems tract (TST), and the maxi-  
 181 mum highstand phase and the lower part of the regressive  
 182 phase correspond to the highstand systems tract (HST).  
 183 The sequence-stratigraphic assignment for the upper part  
 184 of the regressive phase is currently under study, because  
 185 new sequences associated to large paleochannels are de-  
 186 fined in this paper.

187 Taphonomic analysis of the mollusk fauna within the  
 188 transgressive phase (TST), combined with sedimentary  
 189 facies and sequence stratigraphic data, allowed identifying  
 190 a range of paleoenvironments from the deepest mid-inner  
 191 shelf to the shallow intertidal-foreshore (Scasso and del  
 192 Río 1987; del Río et al. 2001). The lower part of the  
 193 regressive phase (HST) is subdivided in low-hierarchy

T-R cycles (probably fourth-order sequences) that start  
 with transgressive surfaces displaying firm or hard-  
 ground trace fossil suites, overlain by either reworked  
 shell beds (coquinas) or strongly bioturbated bioclastic  
 sandstones accumulated in sand bars in a storm-  
 dominated shoreface to inner shelf environment (Scasso  
 and del Río 1987; del Río et al. 2001). These deposits are  
 often cut by deeply erosional surfaces in the middle and  
 upper part of the regressive phase (Fig. 2), which are  
 covered by channel deposits accumulated from the purely  
 fluvial to the tidally dominated outer part of estuaries.  
 These channel deposits are the subject of the present  
 study.

**Methods**

Several channels were identified throughout the study area,  
 and their deposits and discontinuity surfaces described by  
 means of detailed logs and 3-D analysis, with special empha-  
 sis on tracing the discontinuities and the lateral changes in the  
 deposits. The lithologic composition of the sediments was  
 studied with a polarization microscope for the sand fractions  
 and a scanning electron microscope for the mud fractions.

Two examples of paleotidal channels were selected for the  
 present study, namely the Bahía Punta Fósil and Cerro  
 Olazábal paleochannels, because they are nicely exposed on



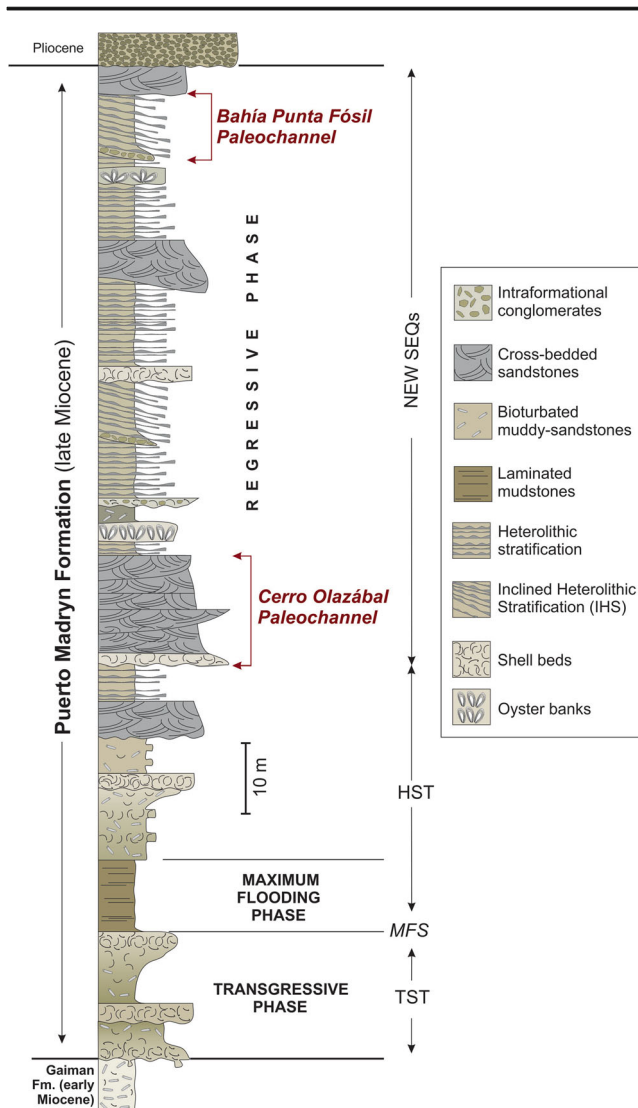


**Fig. 2** Composite stratigraphic column from the Puerto Madryn Formation in the Península Valdés (modified after del Río et al. 2001). From a standard sequence stratigraphic point of view, the transgressive phase of del Río et al. (2001) corresponds to the transgressive systems tract (TST), and the maximum and the lower part of the regressive phases correspond to the highstand systems tract (HST). MFS Maximum flooding surface. The upper part of the regressive phase is currently under revision, and new sequences (NEW SEQs) associated to tidal channels are defined

218 3-D cliffs, the TRSs and sequence boundaries can be traced  
 219 for long distances, and they represent different locations with-  
 220 in the estuarine system. The preserved deposits are mostly  
 221 channel bars and lag conglomerates of different scales, where-  
 222 as inter-channel deposits are rare or absent (compare with  
 223 Scasso et al. 2012). Erosion surfaces are frequently cut into  
 224 older channel deposits. The present study follows the fivefold  
 225 estuary subdivision by Jablonski and Dalrymple (2016) for  
 226 paleoenvironmental assignment in the fluvial-marine transi-  
 227 tion from land to sea: purely fluvial, fluvially dominated/  
 228 tidally influenced, tidally dominated/fluvially influenced,  
 229 and tidally dominated.

**Results**

**Bahía Punta Fósil paleochannel**

232 The Bahía Punta Fósil paleochannel is a large tidal channel  
 233 exposed on the cliff 300 m south of Punta Fósil (42°44'24.97"  
 234 S, 63°38'3.82"W; Fig. 1) where several discontinuity surfaces  
 235 covered by channel deposits were described (Scasso et al.  
 236 2015a). The Bahía Punta Fósil paleochannel axis is oriented  
 237 30° (oblique to the N-S cliff of Fig. 3) and shows a complex  
 238 infilling on top of two erosion surfaces. It constitutes the up-  
 239 permost stratigraphic interval of the Puerto Madryn Formation  
 240 (Fig. 2), on top of a 320-m-thick column of middle to late  
 241 Miocene age lying mostly in the subsurface and recorded in  
 242 an oil well 3 km inland from the cliff (Masiuk et al. 1976;  
 243 Caramés et al. 2004). Several large channels with terrestrial  
 244 vertebrate remains in their channel conglomerate lags were  
 245 identified in the area (Dozo et al. 2010; Scasso et al. 2012;  
 246 Scasso et al. 2015b), lying above marked erosion surfaces  
 247 entrenched up to 50 m deep into the underlying sediments  
 248 (this a minimum value since some erosion surfaces are tracked  
 249 down to the sea level but might go deeper).

250 The infill of the Bahía Punta Fósil paleochannel is com-  
 251 posed (from base to top) of intraclast conglomerate, cross-  
 252 bedded sandstone and decimetric packages of rhythmites  
 253 (Figs. 3 and 4). The intraclast conglomerate lies above an  
 254 irregular erosion surface called here “surface 1” (Fig. 3), and  
 255 it is exclusively composed of whitish mud clasts of gravel to  
 256 block size (Fig. 4a). The top of the intraclast conglomerate  
 257 bed is cut by another, less irregular erosion surface, called here  
 258 “surface 2” (Fig. 3). A 20-m-thick, fining-upward succession  
 259 is developed above surface 2, formed (from base to top) by  
 260 thin conglomerate deposits with parallel stratification and  
 261 gravel-sized bioclasts, intraclasts and bones, well developed  
 262 in the channel thalweg (Fig. 4b). They are covered by large- to  
 263 small-scale cross-bedded sandstones with thick mud drapes  
 264 and mud intraclasts. This facies is thicker along the northern  
 265 margin of the paleochannel and changes laterally to  
 266 decimeter-scale heterolithic beds (Figs. 3 and 4c) that become  
 267 muddier both to the center (to the left in Fig. 3) and upward in  
 268 the channel fill. Both sandy and muddy beds contain fresh,  
 269 abundant shards and pumice.

270 Twenty pairs of several dm- to 1-m-thick rhythmites, each  
 271 formed by a couple of sand- and mud-dominated heterolithic  
 272 beds, were counted in the 18-m-thick interval in the northern  
 273 part of the Bahía Punta Fósil paleochannel infill (Fig. 4c). To  
 274 the south, as the cliff becomes higher, the number of pairs  
 275 increases to about 62, and two discontinuity surfaces in the  
 276 channel fill, mantled with coarser, cross-bedded beds, suggest  
 277 an incomplete record. Within the decimeter-scale beds,  
 278 centimeter-scale sand and mud layers form heterolithic beds  
 279 (Fig. 4d). The centimeter-scale sand layers that compose the  
 280 heterolithic beds show current-ripple lamination with

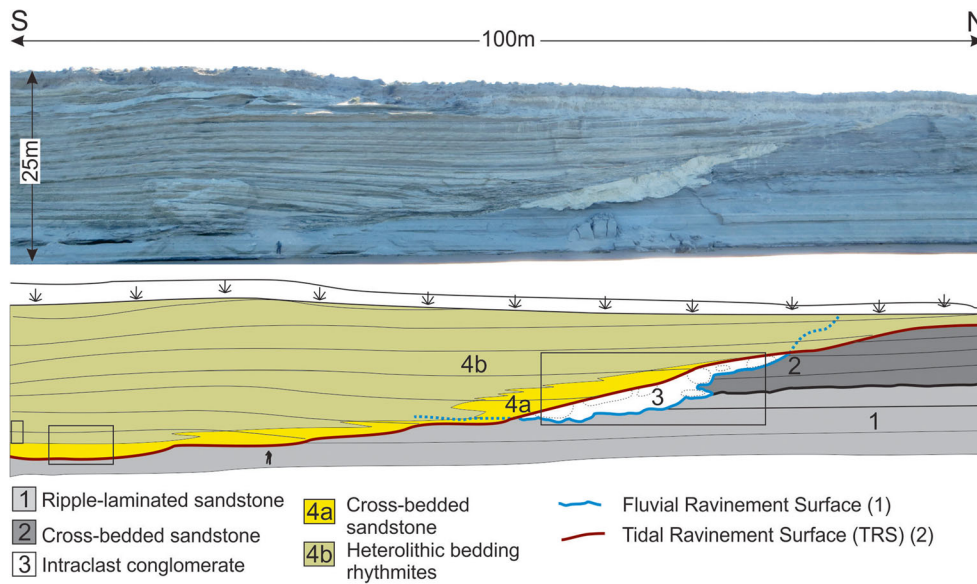


**Fig. 3** Bahía Punta Fossil paleochannel deposits (*above*), and interpretation (*below*). The major erosion surfaces and sedimentary facies are highlighted. The subaerial fluvial ravinement surface (1) is cut by the TRS (2), pointing to a successive entrenchment of the base of the Bahía Punta Fossil paleochannel, which shows a complex infilling

of bioclastic and intraclastic channel lags and decimetric packages of alternating muddy to sandy heterolithic rhythmites forming a fining-upward succession. Rectangles Locations of Fig. 4a (*right*), 4c (*center*), and 4d (*left*). Modified after Scasso et al. (2015a, their Fig. 34)

281 abundant alternating NE and SW paleocurrents (Fig. 4d). The  
 282 NE paleocurrents dominate in the sandy beds and the SW  
 283 paleocurrents dominate in the muddy beds.

284 **Dynamics and evolution of Bahía Punta Fossil**  
 285 **paleochannel**

286 The 20-m-thick, fining-upward succession is thought to rep-  
 287 resent the infilling of a medium- to large-sized tidal channel.  
 288 Surface 1 is interpreted as the bottom erosion surface of an  
 289 incised valley related to a sea-level fall on the basis of its  
 290 irregular erosional shape (Fig. 3) and the paleoenvironment  
 291 of deposition inferred from the overlying deposits. The  
 292 intraclast conglomerate above surface 1 represents erosion  
 293 and block releasing from the channel-cut bank. As blocks  
 294 and clasts show little transport, they must derive from the  
 295 erosion of a bed stratigraphically higher in the succession  
 296 aside the channel, which is not preserved in the cliff probably  
 297 because of recent erosion (Fig. 3). The lack of marine fossils  
 298 together with the steep relief of the channel margin and the  
 299 consolidation of the mud needed for the formation of the  
 300 eroded blocks (Fig. 4a) suggest the conglomerate formed in  
 301 a subaerial environment after the mud beds underwent some  
 302 dehydration in the purely fluvial part of the system.

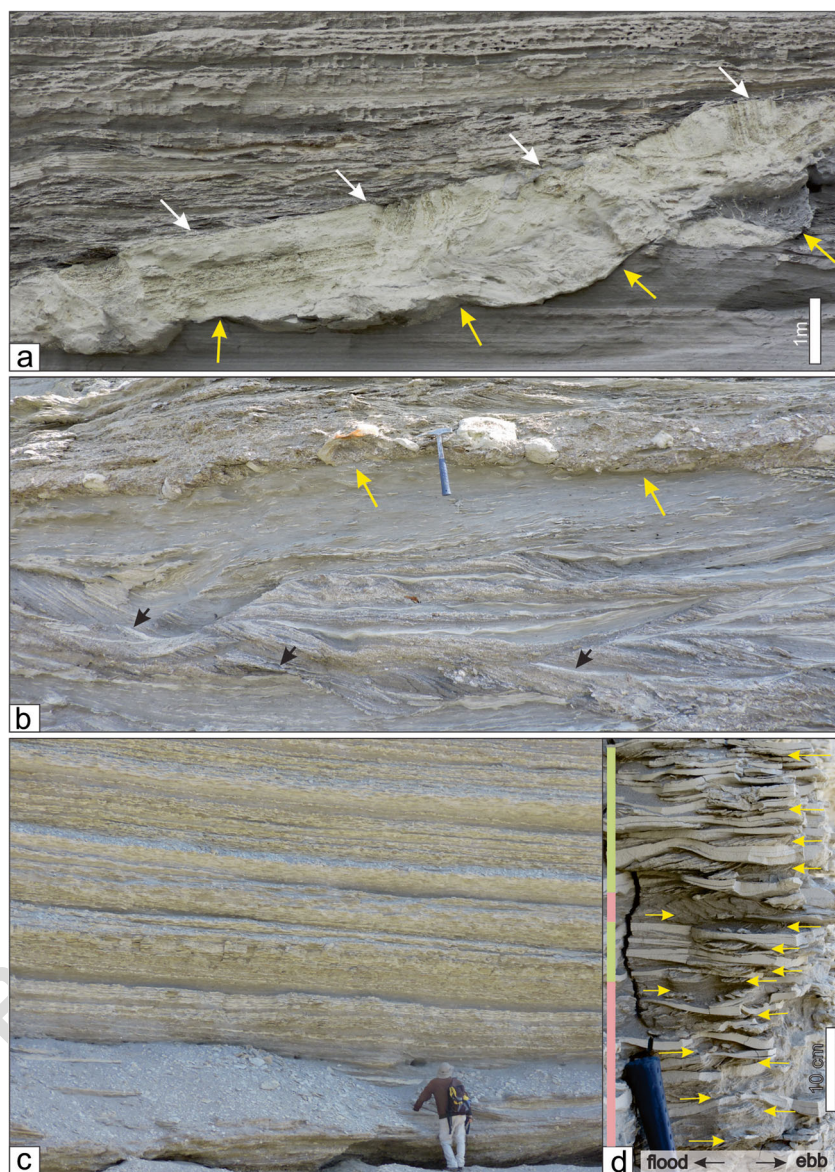
303 Surface 2 cuts surface 1 and delineates the base of the  
 304 channel in a later stage of its evolution (Fig. 3). The bioclastic  
 305 conglomerate is interpreted as a channel lag deposit (cf.  
 306 Flemming et al. 1992; Flemming and Davies 1994) reflecting  
 307 marine influence. Upper-flow parallel bedding in bioclastic  
 308 beds and small dunes of sand and bioclasts reflect strong tidal

currents up to 1 m/s (Flemming and Davies 1994) in the tid- 309  
 ally dominated part of the estuary. The lateral variation in the 310  
 grain size of the rhythmites, from sand-dominated to mud- 311  
 dominated, indicates higher current velocities in the northern, 312  
 more active margin of the paleochannel, suggesting a sinuous 313  
 shape with a meander-like bend. Rhythmic, vertical accretion 314  
 dominates the channel infilling (Figs. 3 and 4a). The 315  
 rhythmites mostly lack marine fossils and bioturbation is rare, 316  
 suggesting deposition under stressing environmental condi- 317  
 tions, which is consistent with brackish waters and high sed- 318  
 imentation rates with high suspended sediment concentrations 319  
 and minimal bioturbation and wave reworking (e.g., Thomas 320  
 et al. 1987; Tessier and Gigot 1989; Dalrymple and MakinoY 321Q1  
 1991). The rhythmites are regarded as typical of macrotidal to 322  
 hypertidal settings (Archer 1995; Tessier 2012), and they are 323  
 better developed with extreme tidal dynamics within trans- 324  
 gressive systems (Archer and Greb 2012). 325

The decimeter-scale heterolithic beds forming rhythmites 326  
 in the Bahía Punta Fossil paleochannel (Fig. 4c) are interpreted 327  
 as seasonal rhythmites whereas the centimeter-scale beds are 328  
 interpreted as neap/spring and semidiurnal/diurnal rhythmites. 329  
 Alternating NE (ebb) and SW (flood) paleocurrents indicate 330  
 numerous current reversals with flood dominance in the mud- 331  
 dier beds and ebb dominance in the sandier beds (Fig. 4d). 332  
 Similar decimeter-scale beds composed of predominantly 333  
 sandy and muddy centimetric layers, with heterolithic and 334  
 ripple bedding, were assigned to seasonal changes in river 335  
 discharge (Van den Berg et al. 2007) in the fluvial-tidal tran- 336  
 sition zone of the estuarine system. During periods of high 337  
 river discharge, sandy layers with ebb-directed paleocurrents 338



**Fig. 4** Facies details of the Bahía Punta Fósil paleochannel. **a** Yellow arrows Subaerial fluvial ravinement surface covered by mud blocks; white arrows TRS. Above this surface, cross-bedded and ripple-laminated sandstones form the tidal channel infill. Modified after Scasso et al. (2015a, their Fig. 34). **b** Channel deposits dominated by cross-bedded sandstones with mud drapes (black arrows) and abundant mud intraclasts. Some layers concentrate bioclasts, rounded intraclasts and transported cetacean bones (yellow arrows); 25 cm long hammer for scale. **c** Seasonal rhythmites formed by muddy (light color) and sandy (dark color) heterolithic beds. Modified after Scasso et al. (2015a, their Fig. 38). **d** Detail of heterolithic rhythmites (pink bars sand-dominated intervals, green bars mud-dominated intervals). Alternating NE (ebb) and SW (flood) paleocurrents indicate numerous current reversals with flood dominance in the muddier intervals. Thick slack water mud drapes reflect high concentrations of suspended volcaniclastic particles. Modified after Scasso et al. (2015a, their Fig. 39)



339 predominate. During periods of low river discharge, the flood  
 340 tide induces a flow directed upstream, which is active during a  
 341 short period of the flood, because of the tidal wave asymmetry  
 342 (e.g., Brenon and Le Hir 1999). Flood-directed ripples covered  
 343 by thick slack water mud drapes reflect high suspended  
 344 mud concentrations in the Bahía Punta Fósil paleochannel.  
 345 The high amounts of fine, reworked ash may have aided in  
 346 the development of a thick fluid mud layer around slack water,  
 347 lacking intercalated sand laminae. Thick mud drapes (up to  
 348 2 cm thick) without intercalated sand laminae are interpreted  
 349 as having been deposited during a single high-water slack  
 350 period (e.g., Shanley et al. 1992). This style of sedimentation  
 351 is typical of an estuary with a turbidity maximum zone and  
 352 may be related to the intrusion of a salt wedge (Van den Berg  
 353 et al. 2007), a process that takes place in the fluvially  
 354 dominated/tidally influenced part of an estuary.

According to the seasonal interpretation for each pair  
 of tidal rhythmites, a 20 year period of continuous sedi-  
 mentation is involved in the 18-m-thick interval devoid of  
 discontinuities (Scasso et al. 2015a). Sedimentation rates  
 as high as 0.9 m/year are estimated. Channel-fill sedi-  
 mentation rates calculated from rhythmites are highly variable  
 and depend on the amount of space available to be filled  
 during deposition (Greb and Archer 1998). In the Bahía  
 Punta Fósil paleochannel, the accommodation space was  
 at least 20 m and high volcaniclastic sediment supply led  
 to rapid aggradation and subsequent channel filling and  
 abandonment. Seasonal periodic changes in the energy of  
 the system are evidenced by the alternating muddier or  
 sandier nature of the beds, which preserved some daily/  
 neap-spring tidal layers within them, but not complete  
 sequences of tidal bundles.

355  
 356  
 357  
 358  
 359  
 360  
 361  
 362  
 363  
 364  
 365  
 366  
 367  
 368  
 369  
 370

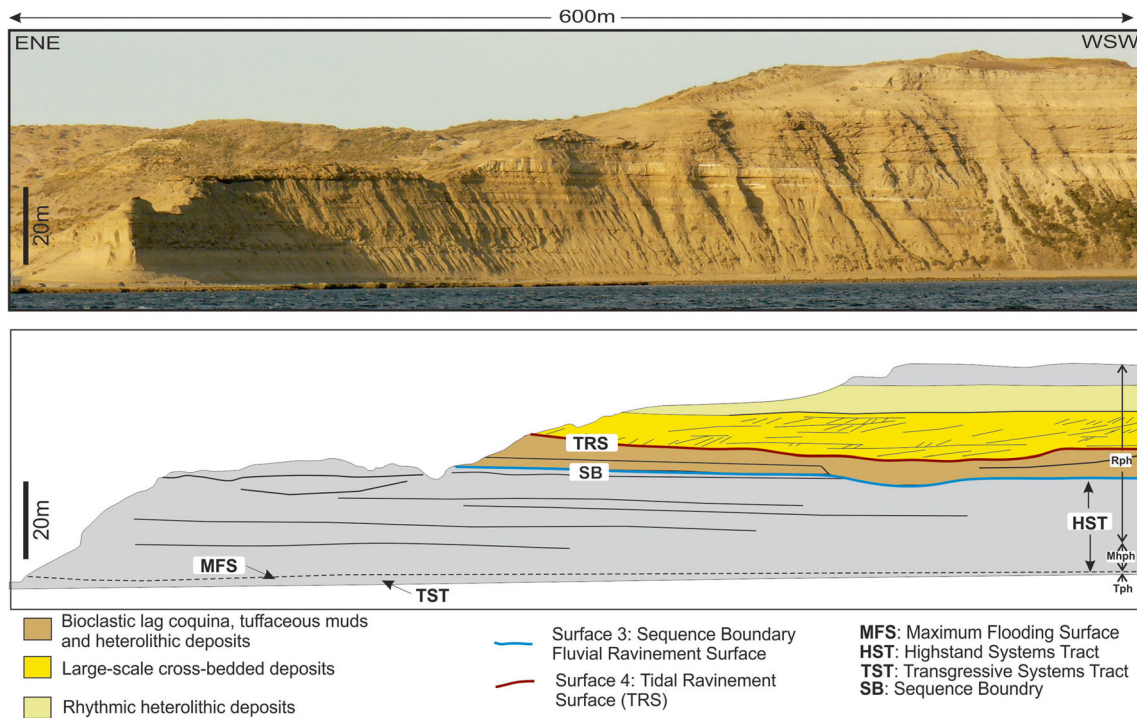


**Fig. 5** Succession at the Cerro Olazábal cliff (*above*) and its interpretation (*below*). The paleochannel deposits and the discontinuity surfaces are highlighted. The regressive (*RPh*), maximum highstand (*Mhph*) and transgressive (*Tph*) phases of del Río et al. (2001) are also indicated

371 **Cerro Olazábal paleochannel**

372 The Cerro Olazábal paleochannel deposits constitute the upper part of the Cerro Olazábal section (42°34'40.63"S, 64°16'14.15"W; Fig. 1), a classical section studied since Florentino Ameghino times (e.g., Feruglio 1949). The paleochannel deposits are part of the regressive phase above the transgressive and maximum flooding phases, also represented in the section (Figs. 2 and 5).

379 The interval studied here starts with a coquina bed with broken and reworked shells above an irregular, high-relief erosion surface, called here “surface 3” (Figs. 2 and 5). The coquina bed is covered by a 2-m-thick, white bed composed of fine, reworked siliceous tuffs (Fig. 6, image A). Together with the underlying surface 3, both can be traced for many km to the south. They pass upward into thin heterolithic deposits and well-sorted, fine-grained sandstones with internal cross-stratification displaying thick mud partings. Large *Ophiomorpha* sp. galleries can be observed in these deposits. At the top of these beds, intense burrowing by a monospecific suite of *Skolithos* sp. penetrates from the overlying bed.

391 A ~0.3-m-thick whitish, massive mudstone bed overlies the cross-bedded, fine-grained sandstones, which are in turn covered by a ~7-m-thick cross-bedded bioclastic sandstone (Fig. 6, image B). The lower contact of these coarse deposits is a surface with erosional relief of several meters cut into the underlying beds, traced for several kilometers along the cliff

and called here “surface 4” (Fig. 5). It is locally irregular and punctuated by traces of *Gastrochaenolites* sp. (Fig. 6, image B). The coarse-grained deposits are composed of shell hash in large-scale trough cross-stratified beds dipping to the west (Fig. 6, images A, B), separated by master bedding planes also dipping to the west. An internal fining-upward trend is observed within this body, which culminates in fine-grained sandstones with medium-scale trough cross-stratification and abundant mud drapes (Fig. 6, image C) or inclined heterolithic stratification (Fig. 6, image A). The uppermost beds in the cliff are packed in two, 10-m-thick intervals of alternating heterolithic and muddy heterolithic bedding (Fig. 5), a lower muddy one, with very thin, weakly bioturbated sandy partitions, and an upper one lying above an irregular surface bioturbated by *Thalassinoides* sp. These upper heterolithic deposits are sand dominated and show intervals of strong bioturbation. To the east of this site, an isolated lenticular oyster bed is intercalated within the heterolithic deposits. It contains large thick-valved oysters, articulated and stuck to each other.

416 **Dynamics and evolution of Cerro Olazábal paleochannel**

417 The basal erosional, high-relief surface 3 can be traced along the coast for 10 km to the south. It separates the underlying marine shelf sediments from the overlying estuarine sediments that represent the channel fill. It was caused by fluvial ravinement during a sea-level fall and it is therefore



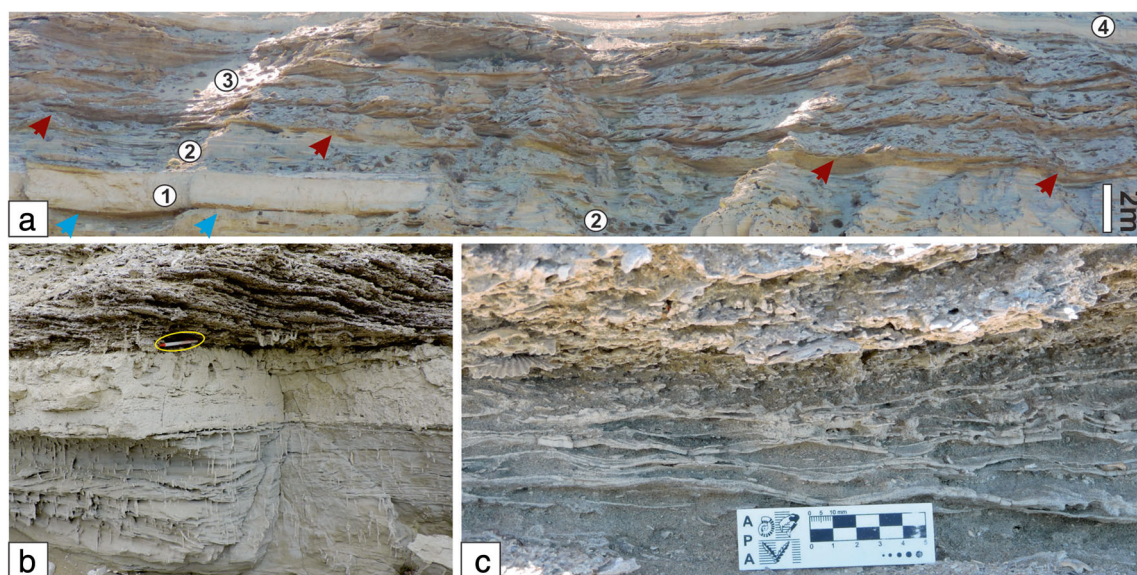


**Fig. 6** Facies details for Cerro Olazábal paleochannel deposits. *Image A* General view of facies: massive volcaniclastic mud bed (1) on top of thin lag coquina overlying surface 3 (blue arrows), a fluvial ravinement surface that constitutes the sequence boundary. This bed is covered by heterolithic deposits (2), which in turn are covered by large-scale cross-bedded sets composed of coarse sandstones and shell hash (3). Paleocurrent directions to the left (W) indicate flood-dominated

conditions. Between facies 2 and 3, surface 4, a TRS, is arrowed (red). Overlying the cross-bedded bioclastic sandstones, a muddy heterolithic bed (4) culminates the channel infill. *Image B* Detail of the base of the large-scale cross-bedded sets overlying surface 4, a TRS bioturbated with *Gastrochaenolites* sp. Pencil (15 cm long) for scale. *Image C* Detail of fine-grained sandstone bed with abundant mud drapes in the upper part of the tidal channel deposits

422 interpreted as a sequence boundary in an incised valley system. The coquina above is interpreted as a marine transgressive lag, associated with marginal marine conditions during initial stages of sea-level rise. The incised valley was later filled with volcaniclastic white muds (Fig. 6, image A), a guide layer that can be also traced for many km to the south. The volcaniclastic muds are interbedded with intertidal-flat and nearshore storm-influenced deposits in the outer tidally dominated part of an estuary.

431 The overlying coarse bioclastic deposits are related to a major tidal channel system lying above a TRS (Fig. 5). Large subaqueous dunes of abraded shells reflect strong tidal currents close to 1 m/s (cf. Flemming and Davies 1994). The channel was incised into the substrate after an increase in tidal current power caused by a relative sea-level rise. Westward (landward), paleocurrents as well as abundant and strongly abraded marine shell remains indicate a landward migration of bedforms in response to the flood tidal current. It is interpreted as a large channel with a flood-dominated tidal point bar with partial “downstream” accretion at the meander ends, formed in the tidally dominated/fluvially influenced part of an estuary, similar to those illustrated by Cuevas Gonzalo and de Boer (1991) and Martinius (2012, their Fig. 18.23) for the Lower Eocene tidalites in the southern Pyrenees (Spain).

447 The muddy to fine-grained sandy heterolithic deposits above the bioclastic beds in the upper part of the channel infill (Figs. 5 and 6, image C) show varying bioturbation intensity

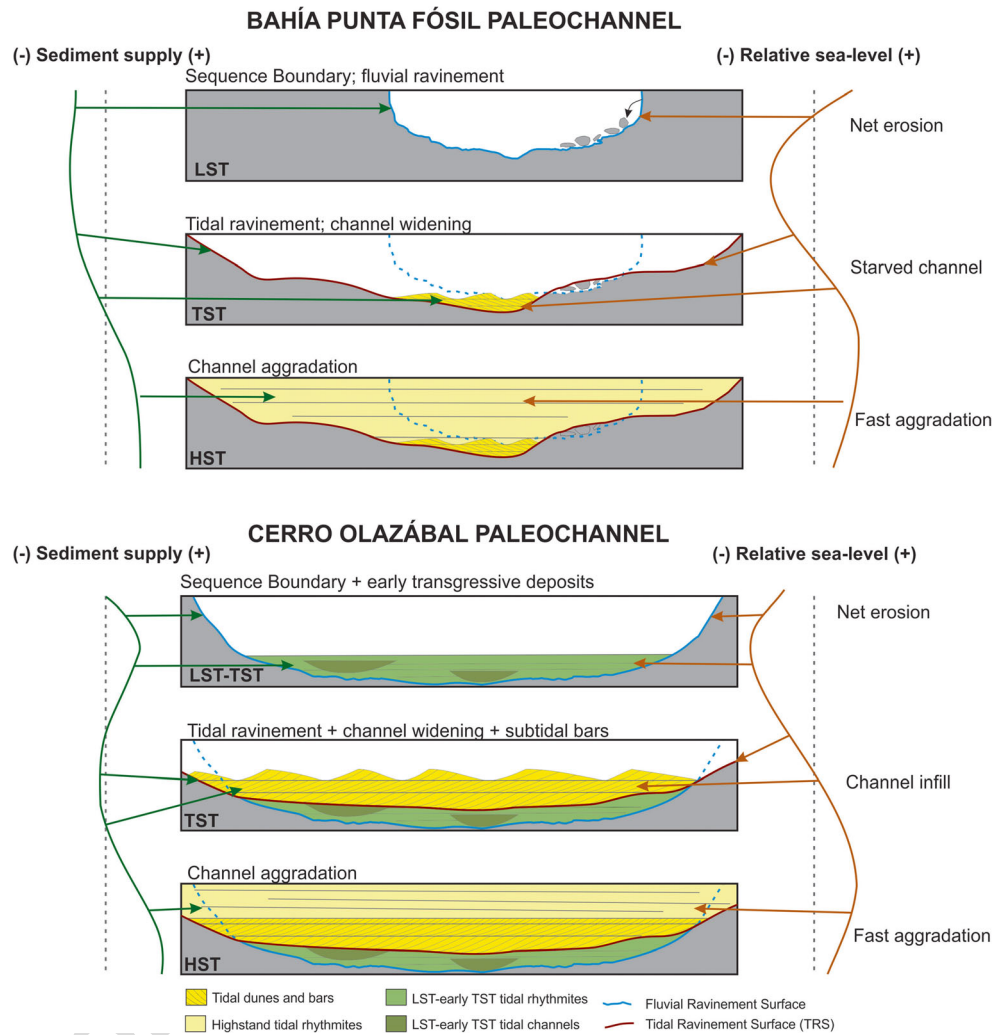
450 resulting from the variation in salinity and sediment input into the channel. High rates of river discharge lowered the salinity and supplied large amounts of sediment, precluding colonization by organisms. On the other hand, lower river discharge favored colonization by marine organisms in the channel, resulting in highly bioturbated beds and oyster biostromes. The 10 m packages of muddy or sandy heterolithics are interpreted as tidal rhythmites within a tidal channel (Greb and Archer 1998), formed in the fluvially dominated/tidally influenced part of an estuary. The lenticular oyster beds intercalated within the heterolithic deposits are mostly preserved in life position and represent an oyster biostrome developed in the shallower parts of the channel under low sedimentation rates. Oyster biostromes were described by Pufahl and James (2006) in similar paleoenvironments.

## Discussion

### Deposits and discontinuities in tidal channels of the Puerto Madryn Formation

468 The Cerro Olazábal and Bahía Punta Fósil paleochannels were selected for the present study because they present most of the typical characteristics of tidal channels in the Puerto Madryn Formation, in addition to well-exposed discontinuities interpreted as fluvial and tidal ravinement surfaces (Figs. 3 and 5). According to the above analysis, the Cerro Olazábal

**Fig. 7** Schematic evolution of the Bahía Punta Fósil and Cerro Olazábal paleochannels (*LST*, *TST* and *HST* lowstand, transgressive and highstand systems tract, respectively)



474 paleochannel deposits accumulated between the lowstand and  
 475 highstand shorelines, mostly in the tidally dominated/fluvially  
 476 influenced part of estuarine tidal channels, as revealed by the  
 477 bioclastic lags rich in marine mollusks, abundant body and  
 478 trace fossils, and flood-dominated paleocurrents (Fig. 7).  
 479 Episodic marine influence evidenced by the trace fossils and  
 480 body fossils may have been associated with seasonal, up-  
 481 stream shifts of the salt wedge in the estuary during dry pe-  
 482 riods (Jablonski and Dalrymple 2016). On the other hand, the  
 483 Bahía Punta Fósil paleochannel deposits indicate sedimenta-  
 484 tion mostly in the fluvially dominated/tidally influenced part  
 485 of the estuary, as revealed by the intraformational conglomer-  
 486 ate lag at the base, ebb-dominated paleocurrents in cross-  
 487 bedded sandstones, and mostly barren seasonal rhythmites.

488 The Bahía Punta Fósil paleochannel deposits accumulated  
 489 landward of the Cerro Olazábal paleochannel, although minor  
 490 and major paleoenvironmental variations are recorded in both  
 491 columns. The former may represent seasonal variations that  
 492 resulted in minor shifts of the estuary zones. The latter are  
 493 associated with sea-level fluctuations that resulted in large

494 paleoenvironmental shifts from purely fluvial to tidally domi-  
 495 nated parts of the estuary (Fig. 7).

496 In addition to the Cerro Olazábal and Bahía Punta Fósil  
 497 paleochannels, other paleochannels have been described for  
 498 the Puerto Madryn Formation (Scasso et al. 2012, 2014,  
 499 2015a). Together, they allow reconstruction of a general pat-  
 500 tern for the tidal-channel infilling in this unit. They display a  
 501 general fining-upward trend similar to the model proposed by  
 502 Choi et al. (2004) for modern Korean tidal flats, with variable  
 503 facies and discontinuities depending on the environmental  
 504 setting. Some paleochannel lags, as those from La Pastosa  
 505 (Fig. 1), are formed by intraformational clasts and blocks,  
 506 and contain terrestrial and freshwater vertebrate remains  
 507 (Scasso et al. 2012). They lie on irregular surfaces deeply  
 508 eroded into the underlying deposits, being interpreted as  
 509 fluvial ravinement surfaces/subaerial unconformities formed by  
 510 fluvial channel erosion during relative sea-level falls in the  
 511 purely fluvial part of the estuary. The conglomerate lags then  
 512 accumulated in the inner segment of incised valleys in the  
 513 “purely fluvial” or “fluvially dominated/tidally influenced”

514 part of the estuary. In other cases (e.g., Scasso et al. 2015a),  
 515 the channel-fill succession starts with upper-flow regime  
 516 parallel-stratified bioclastic lag deposits or large-scale cross-  
 517 bedding. Reworked shells can be completely broken down  
 518 into minute fragments or be preserved in articulated form. In  
 519 some cases, firm to hard-ground fossil traces are found at the  
 520 channel bed and margins. These deposits are assigned to the  
 521 outer segment of incised valleys (sensu Zaitlin et al. 1994) and  
 522 were formed in the tidally dominated/fluvially influenced or in  
 523 the tidally dominated part of the estuary. Under conditions of  
 524 low sediment supply, extensive tidal channel migration pro-  
 525 duced thick bioclastic lag conglomerates and cross-bedded  
 526 bioclastic in-channel bars with dominantly landward-  
 527 oriented paleocurrent bedding formed by flood currents.  
 528 These channel sediments overlie erosion surfaces interpreted  
 529 as TRSs.

530 On top of the lag conglomerates, large arcuate point bars  
 531 with inclined heterolithic stratification (IHS) show rhythmic  
 532 alternation of sandy and muddy beds, which are assigned to  
 533 seasonal changes in river discharge following Jablonski and  
 534 Dalrymple (2016). They were formed in the brackish to fresh-  
 535 water fluvially dominated/tidally influenced part of the estu-  
 536 ary. Varying trace and body fossil contents in the IHS suggest  
 537 varying salinity, river discharge and sediment supply. Closer  
 538 to the channel mouth, in the tidally dominated/fluvially influ-  
 539 enced part of the estuary, IHS bedsets form straight bars, show  
 540 extensive bioturbation and bear mollusk body fossils as de-  
 541 scribed by Scasso et al. (2015a, 2015b) in the Punta Alt (lower  
 542 paleochannel) or Punta Hércules paleochannel (see location in  
 543 Fig. 1).

544 Cross-bedded sandstones with mud drapes are commonly  
 545 found above the IHS deposits, although they can directly over-  
 546 lie the lag conglomerates. They are barren or show little bio-  
 547 turbation, with paleocurrents being mostly directed seaward  
 548 due to dominant ebb currents transporting land-derived sedi-  
 549 ments. These are typical of the fluvially dominated/tidally  
 550 influenced part of the estuary.

551 The upper part of the channel fill is usually composed of  
 552 heterolithic beds with rippled sands and muds of tuffaceous  
 553 composition, and which are interpreted as seasonal rhythmites  
 554 (Scasso et al. 2015a). They lie above any of the underlying  
 555 facies. Their volcanoclastic composition is revealed by abun-  
 556 dant silt- to sand-sized shards present both in the muddy and  
 557 sandy layers of the heterolithic beds. Ash supplied by the  
 558 rivers after large explosive volcanic eruptions on land resulted  
 559 in high inputs of sediment into the system and rapid accumu-  
 560 lation of the rhythmites, with temporary sedimentation rates as  
 561 high as 0.9 m per year. The system was suddenly overloaded  
 562 with volcanoclastic sediments, the tidal channels providing the  
 563 accommodation space for swift deposition and “freezing” of  
 564 the paleorelief through burial. Rapid burial of the overloaded  
 565 channels precluded lateral migration, favored channel avul-  
 566 sion and, for instance, preserved steep channel walls. The

567 fine-grained facies that form the channel infill may show  
 568 well-defined tidal rhythmites that indicate that the channels  
 569 were filled up in a few hundred years. The finest-grained  
 570 muddy heterolithic deposits correspond to the bedload con-  
 571 vergence zone that is located in the tidal freshwater to  
 572 brackish-water zone (or the fluvially dominated/tidally influ-  
 573 enced part of the estuary; Jablonski and Dalrymple 2016),  
 574 probably reflecting mud flocculation and deposition at the  
 575 turbidity maximum (La Croix and Dashtgard 2014). Oyster  
 576 biostromes grew on channel bars and form part of the channel  
 577 system during pauses in sediment supply or minor rises in  
 578 relative sea level (e.g., Scasso et al. 2012). Channel migration  
 579 and associated erosion of bars produced large, monospecific  
 580 oyster accumulations (Fig. 2).

**Fluvial vs. tidal ravinement in sequence boundaries** 581

582 Fluvial ravinement refers here to the process of fluvial erosion  
 583 in a purely fluvial or fluvially dominated part of macro- to  
 584 hypertidal estuaries. Erosion is driven by fluvial currents,  
 585 mostly in meandering channels, in contrast to the tidal  
 586 ravinement that is driven by tidal currents. It differs from the  
 587 fluvial erosion surface or subaerial unconformity because it is  
 588 always linked to an estuary with a large tidal range, and be-  
 589 cause it may occur even during sea-level rise, much like tidal  
 590 ravinelements. By analogy with the TRS, the fluvial ravinement  
 591 surface is defined as “the erosion surface formed in the purely  
 592 fluvial or fluvially dominated part of the estuary, where the  
 593 erosion is driven by fluvial processes”.

594 Repeated lateral migration and vertical incision of estuarine  
 595 channels in the Puerto Madryn Formation produced a com-  
 596 plex pattern of channel fills bounded by erosion surfaces that  
 597 suggest a complex evolution (Fig. 7). These discontinuities  
 598 may theoretically be assigned to autocyclic processes such  
 599 as seasonal channel reactivations or centennial/millennial  
 600 channel migration (Scasso et al. 2012), or allocyclic processes  
 601 such as climatic changes, uplift or secular sea-level variations  
 602 that affected sedimentation within the estuary. In the Puerto  
 603 Madryn Formation, as in many ancient deposits, it is difficult  
 604 to disentangle the origin of the discontinuity surfaces because  
 605 the erosional processes tend to erase them together with the  
 606 older deposits. In addition, the lack of accurate dating methods  
 607 for discriminating short-term processes and limited outcrop  
 608 observation, even in excellent exposures, such as the cliffs  
 609 of the Península Valdés region, preclude a complete 4-D re-  
 610 construction of the geometry and history of the deposits.  
 611 However, detailed observations give some clues about the  
 612 origin and preservation of the sedimentary bodies and discon-  
 613 tinuities between them.

614 The lowermost discontinuities at the base of the main chan-  
 615 nels are regarded as the fluvial ravinement surface that forms  
 616 the lower sequence boundary in incised valleys during  
 617 lowstands, following the ideas of Maynard et al. (2010). On



618 the basis of architectural subsurface reconstructions, these au- 671  
619 thors suggest three criteria for the recognition of incised val- 672  
620 leys between highstand and lowstand shorelines: (1) an elon- 673  
621 gate, channel-shaped incision that can be correlated over a 674  
622 long distance, (2) the base of the incision is a sequence bound- 675  
623 ary, and (3) the sequence boundary can be correlated region- 676  
624 ally on the interfluvial flooding surface/sequence boundary. 677  
625 Their study illustrates incised valleys ranging from tens of 678  
626 meters to a few kilometers in width and from 5 to 60 m in 679  
627 depth that may contain one or multiple channel fills about 5– 680  
628 30 m thick and a few hundred meters wide, similar in size to 681  
629 the channels of the Puerto Madryn Formation. The channel- 682  
630 shaped incision, bounded at its base by an erosion surface, 683  
631 which is the sequence boundary in the case study of 684  
632 Maynard et al. (2010), is also found in the paleochannels of 685  
633 the Puerto Madryn Formation. In fact, these authors suggest 686  
634 that even minor incision within channel deposits may repre- 687  
635 sent sequence boundaries because scouring is related to falls 688  
636 in sea level. 689

637 The studied intervals of the Puerto Madryn Formation suc- 690  
638 cession meet the criteria listed above for incised valleys. 691  
639 Therefore, the deep regional incision below multiple channel- 692  
640 ing and channel migration may be indicative of a marked, 693  
641 relative sea-level fall that promoted the main valley incision. 694  
642 The recurrent channeling in the deposits above the regional 695  
643 incision can be related to high-order sea-level oscillations. 696  
644 However, the characteristics of some erosion surfaces and 697  
645 their overlying deposits relate better to TRSs resulting from 698  
646 deep tidal ravinement in macro- or hypertidal environments. 699  
647 Notably, Zaitlin et al. (1994) stated that the TRS is typically 700  
648 confined to an incised valley and can be mistaken for a second 701  
649 sequence boundary because it is typically overlain by coarse- 702  
650 grained channel deposits. 703

651 TRSs were traditionally assumed to form at the erosional 704  
652 base of a tidal (inlet) channel (Allen and Posamentier 1993) by 705  
653 upward and backward (retrogradational) migration of the es- 706  
654 tuarine barrier/inlet system (Boyd et al. 1992; Dalrymple et al. 707  
655 1992). They cut into the filling of incised valleys in the outer 708  
656 incised valley system (Fig. 1a of Zaitlin et al. 1994) and are 709  
657 part of the transgressive systems tract. As they overlie the 710  
658 erosional surface of incised valleys formed in response to a 711  
659 relative sea-level fall, they constitute the lower sequence 712  
660 boundary (Van Wagoner et al. 1990; Maynard et al. 2010) 713  
661 above the transgressive surface separating the lowstand sys- 714  
662 tems tract from the transgressive systems tract. 715

663 The depth of tidal ravinement is related to the tidal range 716  
664 and current energy in tidal channels within tidally dominated 717  
665 estuaries. Strong currents in some macrotidal or hypertidal 718  
666 settings can erode very deep, eventually cutting the transgres- 719  
667 sive surface (e.g., Allen and Posamentier 1994). Moreover, 720  
668 they may become the main discontinuities within the valley 721  
669 fill (Menier et al. 2006; Chaumillon et al. 2010; Tessier et al. 722  
670 2012; Ahokas et al. 2014). Estuary models for the regressive

part of the Puerto Madryn Formation (Scasso and del Río 671  
1987; del Río et al. 2001; Scasso et al. 2012) fit into the 672  
tide-dominated, open-estuary depositional-coast type of 673  
Chaumillon et al. (2010) that is typically macrotidal to 674  
hypertidal. Strong tidal currents and tidal dominance for the 675  
Puerto Madryn Formation is clearly expressed in the coarse- 676  
grained lag deposits flooring the channels, the abundant scour 677  
surfaces, the presence of large subaqueous dunes and upper- 678  
flow regime sedimentary structures (Scasso et al. 2015a, their 679  
Figs. 28 to 32; compare with Flemming and Davies 1994, and 680  
with the axial deposits of Dalrymple et al. 2012) as well as in 681  
widespread tidal rhythmites, which are typical of macro- to 682  
hypertidal systems (Archer 1995, 2013; Tessier 2012; Archer 683  
and Greb 2012). On the other hand, a macrotidal regime is still 684  
present in the Península Valdés region and it must have been 685  
similar in the late Miocene because only negligible changes in 686  
latitude or shelf width took place. Therefore, well-developed 687  
TRSs resulting from energetic tidal currents should be expect- 688  
ed in the Puerto Madryn Formation. In modern sediment- 689  
starved estuaries of France, the TRS expands upstream, 690  
allowing reworking processes by the TRS to occur all along 691  
the estuary, and leading in some places to a complete erosion 692  
of underlying units (Menier et al. 2006; Chaumillon et al. 693  
2010; Tessier et al. 2012). In the case of the Bahía Punta 694  
Fósil and Cerro Olazábal paleochannels, the TRSs deeply 695  
scour into the transgressive filling of the channels. They get 696  
close to (Cerro Olazábal paleochannel) and eventually cut 697  
(Bahía Punta Fósil paleochannel) the fluvial ravinement sur- 698  
face (Fig. 7). According to the identified paleoenvironments, 699  
these tidal channel deposits occur from the outer part of the 700  
estuary up to the inner, fluvially dominated/tidally influenced 701  
part. 702

703 On the other hand, the Puerto Madryn Formation shows a 704  
transient high sediment input, in response to episodic volcanic 705  
eruptions, interspaced with long periods of low sedimentation 706  
rates and sediment bypass to the offshore Valdés Basin 707  
(Scasso et al. 2015a). The rivers were eventually overloaded 708  
with volcanoclastic sediments, swiftly burying the incised val- 709  
leys and thereby precluding extensive lateral migration of flu- 710  
vial and tidal channels. Consequently, some morphological 711  
features of the channels, like the steep channel walls or the 712  
TRSs, are well preserved through rapid burial and channel 713  
avulsion in a system with pulsed sediment input. Relatively 714  
large accommodation space in the deep channels was provid- 715  
ed by the large tidal range in the Miocene estuaries of the 716  
Puerto Madryn Formation (compare with Tessier 2012). 717

## 717 Conclusions

718 The Puerto Madryn Formation tidal channel infill shows a 719  
general fining-upward succession that starts with 720  
intraformational lag conglomerates formed by

721 intraformational clasts and blocks with terrestrial and freshwa-  
 722 ter vertebrate remains lying on irregular, deeply eroded sur-  
 723 faces interpreted as subaerial unconformities or fluvial  
 724 ravinement surfaces. The latter are regarded as the “erosion  
 725 surface formed in the purely fluvial or fluvially dominated part  
 726 of the estuary, where the erosion is driven by the fluvial pro-  
 727 cesses”. The lag conglomerates are overlain and eventually  
 728 cut (and suppressed) by a TRS covered by high-energy  
 729 bioclastic lag conglomerates composed of marine fossils that  
 730 formed in the “tidally dominated/fluvially influenced” part of  
 731 an estuary under transgressive conditions during times of sea-  
 732 level rise, as shown in the Bahía Punta Fósil and Cerro  
 733 Olazábal examples, but also in several other examples else-  
 734 where in the Península Valdés region. On top of the channel  
 735 lags, large point bars with IHS show rhythmic alternations of  
 736 sandy and muddy beds that are products of seasonal changes  
 737 in river discharge, with varying trace and body fossil content.  
 738 Their arcuate or straight shape, and their fossil contents sug-  
 739 gest deposition in the freshwater, fluvially dominated to the  
 740 saline, tidally dominated part of the estuary. Cross-bedded  
 741 sands with mud drapes and seaward-directed paleocurrents,  
 742 together with dominantly barren sandy to muddy heterolithic  
 743 seasonal rhythmites, accumulated in the channels of the  
 744 fluvially dominated part of the estuary. They make up the  
 745 upper part of the channel infillings, their volcanoclastic com-  
 746 position indicating that ash supplied by rivers after large ex-  
 747 plosive volcanic eruptions on land resulted in high inputs of  
 748 sediment into the system that produced temporary sedimenta-  
 749 tion rates as high as 0.9 m per year. The channel system was  
 750 overloaded and the accommodation space provided by the  
 751 large channels was swiftly filled up by volcanoclastic sedi-  
 752 ments, preserving the morphology of the tidal channels and  
 753 TRSs through burial.

754 The channel deposits of the Puerto Madryn Formation fit  
 755 into the tide-dominated, open-estuary depositional-coast type  
 756 of Chaumillon et al. (2010), which is typically macrotidal to  
 757 hypertidal. A large tidal range is also suggested by the pres-  
 758 ence of abundant tidal rhythmites and coarse sediments de-  
 759 posited under upper-flow regime conditions within the tidal  
 760 channels. Therefore, well-developed TRSs resulting from en-  
 761 ergetic tidal currents deeply scoured into the transgressive  
 762 channel fills, eventually cutting the fluvial ravinement surface  
 763 and becoming the sequence boundary. This occurred during  
 764 long periods of low sedimentation rates, extended channel  
 765 migration and sediment bypassing, whereas transient, high  
 766 volcanoclastic input interrupted that process through sediment  
 767 overloading and rapid burial under transgressive conditions  
 768 during times of sea-level rise, as shown in the Bahía Punta  
 769 Fósil and Cerro Olazábal examples, but also in several other  
 770 examples elsewhere in the Península Valdés region.

771 The TRS extended upstream to the inner part of the estuary,  
 772 cutting deeply into the channel fill and eventually into the  
 773 fluvial ravinement surface or the subaerial erosion surface.

The tidal channels of the Puerto Madryn Formation constitute 774  
 a unique example of estuarine sedimentation under pulsed 775  
 high and low sediment supply in a macrotidal to hypertidal 776  
 estuary. 777

**Acknowledgments** Thanks go to the owners and workers of many 778  
 Estancias and touristic settlements of the Península Valdés. Special thanks 779  
 are extended to Claudia Villegas from the Punta Delgada Hotel, Teresa 780  
 Dozo and Julio César (Bocha) Rúa (CENPAT-CONICET) for field sup- 781  
 port, and the Administración del Área Natural Protegida Península Valdés 782  
 for permission to work in the area. Funding by CONICET, ANPCYT and 783  
 UBACYT is greatly acknowledged. Two anonymous reviewers substan- 784  
 tially contributed to the improvement of this paper. 785  
 786

**Compliance with ethical standards** 787

**Conflict of interest** The authors declare that there is no conflict of 788  
 interest with third parties. 789

790

**References** 791

Ahokas JM, Nystuen JP, Martinius AW (2014) Depositional dynamics 793  
 and sequence development in a tidally influenced marginal marine 794  
 basin: Early Jurassic Neill Klintner Group, Jameson Land Basin, East 795  
 Greenland. In: Martinius AW, Ravnås R, Howell JA, Steel RJ, 796  
 Wonham JP (eds) From depositional systems to sedimentary succes- 797  
 sions on the Norwegian Continental Margin. *Int Assoc Sedimentol* 798  
*Spec Publ* 46:291–338 799

Allen GP, Posamentier HW (1993) Sequence-stratigraphy and facies 800  
 model of an incised valley fill: the Gironde Estuary, France. *J Sed* 801  
*Petrol* 63:378–391 802

Allen GP, Posamentier HW (1994) Transgressive facies and sequence 803  
 architecture in mixed tide- and wave-dominated incised valleys: 804  
 example from the Gironde Estuary, France. In: Dalrymple RW, 805  
 Boyd R, Zaitlin BA (eds) *Incised valley systems: Origin and sedi-* 806  
*mentary sequences.* *SEPM Spec Publ* 51:225–240 807

Archer AW (1995) Modeling of cyclic tidal rhythmites based on a range 808  
 of diurnal to semidiurnal tidal-station data. *Mar Geol* 123:1–10 809

Archer AW (2013) World’s highest tides: Hypertidal coastal systems in 810  
 North America, South America and Europe. *Sed Geol* 284–285:1– 811  
 25 812

Archer AW, Greb SF (2012) Hypertidal facies from the Pennsylvanian 813  
 Period: Eastern and Western Interior Coal Basins, USA. In: Davis 814  
 RA Jr, Dalrymple RW (eds) *Principles of tidal sedimentology.* 815  
 Springer, Heidelberg, pp 421–436 816

Ashley GM, Sheridan RE (1994) Depositional model for valley fills on a 817  
 passive continental margin. In: Dalrymple RW, Boyd R, Zaitlin BA 818  
 (eds) *Incised valley systems: Origin and sedimentary sequences.* 819  
*SEPM Spec Publ* 51:285–301 820

Boyd R, Dalrymple RW, Zaitlin BA (1992) Classification of coastal sed- 821  
 imentary environments. *Sed Geol* 80:139–150 822

Brenon I, Le Hir P (1999) Modelling the turbidity maximum in the Seine 823  
 estuary (France): identification of formation processes. *Estuar Coast* 824  
*Shelf Sci* 49:525–544 825

Caramés A, Malumíán N, Nánñez C (2004) Foraminíferos del Paleógeno 826  
 del Pozo Península Valdés (PV. es-1), Patagonia septentrional, 827  
 Argentina. *Ameghiniana* 41(3):461–474 828

- 829 Chaumillon E, Tessier B, Reynaud J-Y (2010) Stratigraphic records and  
830 variability of incised valleys and estuaries along French coasts. *Bull*  
831 *Soc géol Fr* 181(2):75–85
- 832 Choi KS, Dalrymple RW, Chun SS, Kim SP (2004) Sedimentology of  
833 modern, inclined heterolithic stratification (IHS) in the macrotidal  
834 Han River delta, Korea. *J Sed Res* 74:677–689
- 835 Cuevas Gonzalo M, de Boer PL (1991) Tide-influenced fluvial deposits;  
836 examples from Eocene of the southern Pyrenees. In: Marzo M,  
837 Puigdefàbregas C (eds) *Guidebook to the 4th International*  
838 *Conference on Fluvial Sedimentology*. Publicacions del Servei  
839 *Geològic de Catalunya*
- 840 Cuitiño JI, Scasso RA (2013) Reworked pyroclastic beds in the early  
841 Miocene of Patagonia: reaction in response to high sediment supply  
842 during explosive volcanic events. *Sed Geol* 289:194–209
- 843 Dalrymple RW, Makino Y ZBA (1991) Temporal and spatial patterns of  
844 rhythmite deposition on mud flats in the macrotidal, Cobequid Bay–  
845 Salmon River estuary, Bay of Fundy, Canada. In: Smith DG,  
846 Reinson GE, Zaitlin BA, Rahmani RA (eds) *Clastic tidal sediment-*  
847 *ology*. *Can Soc Petrol Geol Memoir* 16:137–160
- 848 Dalrymple RW, Zaitlin BA, Boyd R (1992) Estuarine facies models:  
849 conceptual basis and stratigraphic implications. *J Sed Petrol* 62:  
850 1130–1146
- 851 Dalrymple RW, Mackay DA, Ichaso AA, Choi KS (2012) Processes,  
852 morphodynamics, and facies of tide-dominated estuaries. In: Davis  
853 RA Jr, Dalrymple RW (eds) *Principles of tidal sedimentology*.  
854 Springer, Heidelberg, pp 79–107
- 855 del Río CJ (2004) Tertiary marine molluscan assemblages of eastern  
856 Patagonia (Argentina): a biostratigraphic analysis. *J Paleontol*  
857 78(6):1097–1122
- 858 del Río CJ, Martínez SA, Scasso RA (2001) Nature and origin of spec-  
859 tacular marine Miocene shell beds of Northeastern Patagonia  
860 (Argentina): paleoecological and bathymetric significance. *Palaios*  
861 16:3–25
- 862 Dozo MT, Bouza P, Monti A, Palazzesi L, Barreda V, Massaferro G,  
863 Scasso RA, Tambussi CP (2010) Late Miocene continental biota  
864 in Northeastern Patagonia (Península Valdés, Chubut, Argentina).  
865 *Palaeogeogr Palaeoclimatol Palaeoecol* 297:100–109
- 866 Feruglio E (1949) *Descripción Geológica de la Patagonia*. Dirección  
867 *General de Yacimientos Petrolíferos Fiscales*, Buenos Aires
- 868 Flemming BW, Davies RA Jr (1994) Holocene evolution,  
869 morphodynamics and sedimentology of the Spiekeroog barrier is-  
870 land system (southern North Sea). *Senckenberg marit* 24:117–155
- 871 Flemming BW, Schubert H, Hertweck G, Müller K (1992) Bioclastic tidal  
872 channel lag deposits: a genetic model. *Senckenberg marit* 22:109–  
873 129
- 874 Greb SF, Archer AW (1998) Annual sedimentation cycles in rhythmites  
875 of carboniferous tidal-channels. In: Alexander CR, Davies RA,  
876 Henry VJ (eds) *Tidalites, processes and products*. *SEPM Spec*  
877 *Publ* 61:75–83
- 878 Haller MJ (1979) *Estratigrafía de la región al poniente de Puerto Madryn,*  
879 *provincia del Chubut, República Argentina*. In: 7 Congreso  
880 *Geológico Argentino Actas* 1, pp 285–297, Neuquén
- 881 Jablonski BVJ, Dalrymple RW (2016) Recognition of strong seasonality  
882 and climatic cyclicality in an ancient, fluvially dominated, tidally in-  
883 fluenced point bar: Middle McMurray Formation, Lower Steepbank  
884 River, north-eastern Alberta. *Canada Sedimentology*. doi:10.1111  
885 /sed.12228
- 886 La Croix AD, Dashtgard S (2014) Of sand and mud: sedimentological  
887 criteria for identifying the turbidity maximum zone in a tidally in-  
888 fluence river. *Sedimentology* 61:1961–1981
- 889 Marengo H (2015) Neogene micropaleontology and stratigraphy of  
890 Argentina. The Chaco-Paranense basin and the Península de  
891 Valdés. *Springer Briefs in Earth System Sciences*. South America  
892 and the Southern Hemisphere. Springer, Heidelberg
- 893 Marinelli RV, Franzín HJ (1996) Cuencas de Rawson y Península de  
894 Valdés. In: Ramos VA, Turic MA (eds) *Geología y recursos de la*  
*Plataforma Continental Argentina*. 13 Congreso Geológico  
Argentino y 3 Congreso de Exploración de Hidrocarburos.  
*Relatorio* 9:159–169
- Martínez S, del Río CJ (2002) Las provincias malacológicas miocenas y  
recientes del Atlántico sudoccidental. *Anales Biología* 24:121–130
- Martinius AW (2012) Contrasting styles of siliciclastic tidal deposits in a  
developing thrust-sheet-top basins – The Lower Eocene of the  
Central Pyrenees (Spain). In: Davis RA Jr, Dalrymple RW (eds)  
*Principles of tidal sedimentology*. Springer, Heidelberg, pp 473–  
506. doi:10.1007/978-94-007-0123-6\_18
- Masiuk V, Becker D, García Espiasse A (1976) *Micropaleontología y*  
*sedimentología del Pozo YPF Ch. PV es-1 (Península de Valdez)*  
*Provincia del Chubut, República Argentina*. *Importancia y*  
*correlaciones*. ARPEL 24, Yacimientos Petrolíferos Fiscales
- Maynard JR, Feldman HR, Alway R (2010) From bars to valleys: the  
sedimentology and seismic geomorphology of fluvial to estuarine  
incised-valley fills of the Grand Rapids Formation (Lower  
Cretaceous) Iron River Field, Alberta, Canada. *J Sed Res* 80:611–  
638
- Menier D, Reynaud J-Y, Proust J-N, Guillocheau F, Guennoc P, Bonnet S,  
Tessier B, Goubert E (2006) Basement control on shaping and  
infilling of valleys incised at the southern coast of Brittany,  
France. In: Dalrymple RW, Leckier DA, Tillman RW (eds) *Incised*  
*valleys in time space*. *SEPM Spec Publ* 85:37–96
- Palazzesi L, Barreda V (2004) Primer registro palinológico de la  
Formación Puerto Madryn, Mioceno de la provincia del Chubut,  
Argentina. *Ameghiniana* 41:355–362
- Pufahl PK, James NP (2006) Monospecific Pliocene oyster buildups,  
Murray Basin, South Australia: brackish water end member of the  
reef spectrum. *Palaeogeogr Palaeoclimatol Palaeoecol* 233:11–33
- Scasso RA, del Río CJ (1987) Ambiente de sedimentación, estratigrafía y  
proveniencia de la secuencia marina del Terciario superior de la  
región de península de Valdés. *Rev Asoc Geol Arg* 42(3-4):291–321
- Scasso RA, McArthur JM, del Río CJ, Martínez S, Thirlwall MF (2001)  
<sup>87</sup>Sr/<sup>86</sup>Sr Late Miocene age of fossil molluscs in the “Entreterriense”  
of the Valdés Peninsula (Chubut, Argentina). *J South Am Earth Sci*  
14:319–329
- Scasso RA, Cuitiño JI, Escapa I (2010) Mesozoic-Cenozoic basins of  
Central Patagonia with emphasis in their tidal systems. In: del  
Papa C, Astini R (eds) *Field Excursion Guidebook, 18th Int*  
*Sedimentological Congr, Mendoza, Argentina, FE-C9*, pp 1–43
- Scasso RA, Dozo MT, Cuitiño JI, Bouza P (2012) Meandering tidal-  
fluvial channels and lag concentration of terrestrial vertebrates in  
the fluvial-tidal transition of an ancient estuary in Patagonia. *Latin*  
*Am J Sed Basin Analysis* 19(1):27–45
- Scasso RA, Cuitiño JI, Dozo T, Vrba AV (2014) Análisis de  
discontinuidades en el Rionegrense de la Península Valdés.  
*Abstracts 14 Reunión Argentina de Sedimentología, Puerto*  
*Madryn, Chubut*
- Scasso RA, Cuitiño JI, Bouza PJ (2015a) Miocene and modern tidal  
deposits of the Valdes Peninsula. *Field Guide, Field Trip 3, 9th Int*  
*Conf Tidal Sedimentology, Puerto Madryn, Argentina*
- Scasso RA, Cuitiño JI, Dozo MT (2015b) Incised valleys and channel  
fills in the Puerto Madryn Formation (Miocene) of Península Valdés,  
Patagonia, Argentina. In: 9th Int Conf Tidal Sedimentology, Actas,  
pp 156–159. Puerto Madryn, Argentina
- Shanley KW, McCabe PJ, Hattinger RD (1992) Tidal influence in  
Cretaceous fluvial strata from Utah, USA: a key to sequence strati-  
graphic interpretation. *Sedimentology* 39:905–930
- Smith GA (1991) Facies sequences and geometries in continental  
volcaniclastic sediments. In: Fisher RV, Smith GA (eds)  
*Sedimentation in volcanic settings*. *SEPM Spec Publ* 45:109–121
- Tessier B (2012) Stratigraphy of tide-dominated estuaries. In: Davis RA  
Jr, Dalrymple RW (eds) *Principles of tidal sedimentology*. Springer,  
Heidelberg, pp 109–128. doi:10.1007/978-94-007-0123-6\_6

960	Tessier B, Gigot P (1989) A vertical record of different tidal cyclicities -	deposits of the Rhine and Meuse. <i>Neth J Geosci Geol Mijnb</i> 86:	974
961	an example from the Miocene marine molasse of Digne.	287–306	975
962	<i>Sedimentology</i> 36:767–776		
963	Tessier B, Billeaud I, Sorrel P, Delsinne N, Lesueur P (2012) Infilling	Van Wagoner JC, Mitchum RM, Campion KM, Rahmanian VD (1990)	976
964	stratigraphy of macrotidal tide-dominated estuaries. Controlling	Siliciclastic sequence stratigraphy in well logs, cores and outcrops.	977
965	mechanisms: Sea-level fluctuations, bedrock morphology, sediment	<i>AAPG Methods in Exploration Series</i> , vol 7	978
966	supply and climate changes (The examples of the Seine estuary and	Zaitlin BA, Dalrymple RW, Boyd R (1994) The stratigraphic organization	979
967	the Mont-Saint-Michel Bay, English Channel, NW France). <i>Sed</i>	of incised valley systems associate with relative sea level changes.	980
968	<i>Geol</i> 279:62–73	In: Dalrymple RW, Boyd R, Zaitlin BA (eds) <i>Incised valley systems:</i>	981
969	Thomas RG, Smith DG, Wood JM, Visser J, Calverley-Range EA, Koster	Origin and sedimentary sequences. <i>SEPM Spec Publ</i> 51:45–60	982
970	EH (1987) Inclined heterolithic stratification – Terminology, de-	Zinsmeister W, Marshall LG, Drake R, Curtis G (1981) First radioisotope	983
971	scription and significance. <i>Sed Geol</i> 53:123–179	(potassium-argon) age of marine Neogene Río Negro Beds in north-	984
972	Van den Berg JH, Boersma JR, van Gelder A (2007) Diagnostic sediment-	eastern Patagonia, Argentina. <i>Science</i> 212:440	985
973	ary structures of the fluvial-tidal transition zone – Evidence from		
986			

UNCORRECTED PROOF



## AUTHOR QUERY

### **AUTHOR PLEASE ANSWER QUERY.**

- Q1. Dalrymple et al. 1991 has been changed to Dalrymple and MakinoY 1991 as per the reference list. Please check if okay.

UNCORRECTED PROOF